

Received: 2019.09.29

Accepted: 2019.11.20

Available online: 2020.01.22

Published: 2020.03.14

# MicroRNA-143 Increases Oxidative Stress and Myocardial Cell Apoptosis in a Mouse Model of Doxorubicin-Induced Cardiac Toxicity

Authors' Contribution:

Study Design A  
Data Collection B  
Statistical Analysis C  
Data Interpretation D  
Manuscript Preparation E  
Literature Search F  
Funds Collection G

ABCDE **Xin-Qiang Li**  
AEF **Ya-Kui Liu**  
BCDE **Jun Yi**  
CDE **Jia-Shou Dong**  
BCD **Pan-Pan Zhang**  
BCD **Lei Wan**  
CD **Kui Li**

Department of Thoracic and Cardiovascular Surgery, Jingmen First Peoples' Hospital, Jingmen, Hubei, P.R. China

**Corresponding Author:** Ya-Kui Liu, e-mail: hubeilyk@163.com  
**Source of support:** Departmental sources

**Background:** Oxidative stress and myocardial apoptosis are features of doxorubicin-induced cardiac toxicity that can result in cardiac dysfunction. Previous studies showed that microRNA-143 (miR-143) was expressed in the myocardium and had a role in cardiac function. This study aimed to investigate the effects and possible molecular mechanisms of miR-143 on oxidative stress and myocardial cell apoptosis in a mouse model of doxorubicin-induced cardiac toxicity.


**Material/Methods:** Mice underwent intraperitoneal injection of doxorubicin (15 mg/kg) daily for eight days to develop the mouse model of doxorubicin-induced cardiac toxicity. Four days before doxorubicin administration, a group of mice was pretreated daily with a miR-143 antagonist (25 mg/kg/day) for four consecutive days by tail vein injection. The study included the use of a miR-143 antagomir, or anti-microRNA, an oligonucleotide that silenced endogenous microRNA (miR), and an agomir to miR-143, and also the AKT inhibitor, MK2206. Quantitative real-time polymerase chain reaction (qRT-PCR) and immunoblot analysis were used to measure mRNA and protein expression, respectively.

**Results:** Doxorubicin treatment increased the expression of miR-143, which was reduced by the miR-143 antagomir. Overexpression of miR-143 increased doxorubicin-induced myocardial apoptosis and oxidative stress. The use of the miR-143 antagomir significantly activated protein kinase B (PKB) and AKT, which were reduced in the presence of the AKT inhibitor, MK2206. However, the use of the miR-143 antagomir further down-regulated AKT phosphorylation following doxorubicin treatment and increased AKT activation.

**Conclusions:** In a mouse model of doxorubicin-induced cardiac toxicity, miR-143 increased oxidative stress and myocardial cell apoptosis following doxorubicin treatment by inhibiting AKT.

**MeSH Keywords:** **Apoptosis • Doxorubicin • Oxidative Stress**

**Full-text PDF:** <https://www.medscimonit.com/abstract/index/idArt/920394>

 3720

 1

 6

 43



## Background

Doxorubicin is a broad-spectrum anthracycline chemotherapy agent that has been commonly used in the treatment of solid tumors, lymphoma, and leukemia. However, the clinical use of doxorubicin is associated with side-effects that include cardiac toxicity [1,2]. Doxorubicin-induced cardiac toxicity has multiple mechanisms, including DNA damage, abnormal protein processing, reduced vascularity, and activation of innate immune responses [3–5]. However, emerging evidence suggests that the induction of free radicals is the main mechanism for doxorubicin-induced cardiac toxicity [3–5]. Doxorubicin has a specific affinity for cardiomyocytes and may be retained in the inner membrane of mitochondria, resulting in changes to mitochondrial ultrastructure and function, leading to the generation of reactive oxygen species (ROS) and cell apoptosis [6].

MicroRNAs (miRNAs) are gene regulators that are involved in many cell processes and have critical roles in post-transcriptional regulation [7]. Previous studies have shown that miRNAs are associated with the progression of doxorubicin-induced cardiac toxicity and that these effects may be identified by measuring sensitive biomarkers for cardiac toxicity [8,9]. A previous study has shown that microRNA-146a (miR-146a) was upregulated in cardiomyocytes following doxorubicin treatment and that the upregulation of miR-146a promoted cell death in doxorubicin-induced cardiac toxicity by targeting the ERBB4 gene [9]. Recently, Zhao et al. also showed that overexpression of miR-140-5p significantly suppressed NF-E2-related factor 2 (Nrf2) and sirtuin 2 (SIRT2) to increase doxorubicin-induced oxidative stress and cardiac dysfunction [10].

Previous studies have identified microRNA-143 (miR-143) as a molecular regulator in cell proliferation, apoptosis, and cell migration [11–13]. Overexpression of miR-143 inhibits the progression of the cell-cycle and increases the apoptotic rate of tumor cells [14,15]. Also, miR-143 is expressed in endothelial cells (ECs) and vascular smooth muscle cells (VSMCs), and has roles in modulating angiogenesis and the communication between ECs and VSMCs [11,12,16]. However, Deacon et al. showed that miR-143 was also abundantly expressed in the myocardium and was essential for cardiac function and morphogenesis [17]. Overexpression of miR-143 promoted the spread of mitochondrial membrane potential and increased ischemia-induced cardiac impairment, but miR-143 silencing prevented hydrogen peroxide-mediated cardiac progenitor cell apoptosis [18,19].

Therefore, this study aimed to investigate the effects and possible molecular mechanisms of miR-143 on oxidative stress and myocardial cell apoptosis in a mouse model of doxorubicin-induced cardiac toxicity.

## Material and Methods

### Materials

The antagomir and agomir of miR-143 and the negative controls were purchased from RiboBio (Guangzhou, China). Doxorubicin was obtained from Sigma-Aldrich (St. Louis MO, USA). Measurement of levels of malonaldehyde (MDA), and the antioxidant, glutathione (GSH), and the activity of superoxide dismutase (SOD) and NADPH oxidase (NOX) were detected using kits and were performed at the Nanjing Jiancheng Bioengineering Institute. The levels of 3-nitrotyrosine (3-NT) and 4-hydroxynonenal (4-HNE) were quantified using enzyme-linked immunosorbent assay (ELISA) kits that were purchased from Abcam (Cambridge, MA, USA). The terminal deoxynucleotidyl transferase-mediated dUTP nick end-labeling (TUNEL) fluorescence detection kit was purchased from Merck Millipore (Burlington, MA, USA). The cell counting kit-8 (CCK-8) assay and dichloro-dihydro-fluorescein diacetate (DCFH-DA) were obtained from Beyotime Biotechnology (Shanghai, China). The following primary antibodies were obtained from Cell Signaling Technology (Danvers, MA, USA) and included antibodies to phosphorylated P38 MAP kinase (P-P38, Thr180/Tyr182), total P38 (T-P38), P-extracellular signal-regulated kinase (P-ERK, Thr202/Tyr204), T-ERK, protein kinase C epsilon (PKCε), P-protein kinase B (P-AKT, Ser473), T-AKT, and glyceraldehyde-3-phosphate dehydrogenase (GAPDH).

### The mouse model of doxorubicin-induced cardiac toxicity and the treatment groups

The animal protocols used in this study were approved by the Ethics Committee of Jingmen First Peoples' Hospital and were in accordance with the 1996 Guide for the Care and Use of Laboratory Animals from the National Institutes of Health (NIH).

Adult male C57BL/6 mice, between 8–10 weeks old, with a bodyweight of 23–27 g, were obtained from Huafukang Bioscience Co., Ltd. (Beijing, China) and were maintained with free access to food and drink for more than one week before the study commenced. Mice were given a daily intraperitoneal injection of doxorubicin (15 mg/kg) for eight days to develop the doxorubicin-induced cardiac toxicity model, or normal saline (NS) in the control group, as previously described [3,4]. Four days before doxorubicin administration, the mice were pre-treated daily with the miR-143 antagomir, the miR-143 agomir, and the negative controls (25 mg/kg/day) for four consecutive days, by tail vein injection, as previously described [18].

The AKT inhibitor, MK2206 (SelleckChem, Houston, TX, USA) was administered to mice by intraperitoneal injection at a dose of 66 mg/kg every other day, commencing on the fourth day before doxorubicin treatment, as previously described [20].

**Table 1.** Primer sequences for quantitative real-time polymerase chain reaction (qRT-PCR).

Gene	Species	Forward primer (5'→3')	Reverse primer (5'→3')
miR-143	Mouse	GGTGAGATGAAGCACT	GCAATTGCACTGGATA
BCL-2	Mouse	GTCGCTACCGTCGTGACTTC	CAGACATGCACCTACCCAGC
BAX	Mouse	TGAAGACAGGGGCCTTTTGG	AATTCGCCGGAGACACTCG
miR-143	Rat	GGTGAGATGAAGCACTGTA	TCGGCAATTGCACTGGATA
BCL-2	Rat	CTGTGGATGACTGAGTACCTGAAC	AGAGACAGCCAGGAGAAATCAAAC
BAX	Rat	TCATGAAGACAGGGGCCTTTT	CAATCATCCTCTGCAGCTCCA

One week before doxorubicin treatment, the mice received an intramyocardial injection of the active AKT adenoviral vector (Ad-ca.Akt) (Hanbio Biotechnology Co., Shanghai, China) to overexpress AKT in the myocardium, or Ad-Gfp as the control, as previously described [21]. Briefly, the mouse thoracic cage was surgically opened at the third intercostal space, followed by intramyocardial injection with Ad-ca.Akt or Ad-Gfp ( $1 \times 10^9$ ) with the adenoviral genome particles diluted in 15  $\mu$ l of normal saline. Injections were performed at three locations in the left ventricle. Eight days following doxorubicin treatment, all mice underwent echocardiography and cardiac catheterization measurements. The mice were observed weekly for five weeks after doxorubicin injection to determine the survival rate. At the end of the study, the mice were euthanized, and the heart was removed from each mouse for further studies.

#### Echocardiography and cardiac catheterization

The mice were placed on a heating pad to maintain body temperature and were anesthetized using 0.5–1.0% isoflurane followed by noninvasive echocardiography using the Vevo 770™ High-Resolution Imaging System (VisualSonics, Toronto, ON, Canada) to evaluate cardiac structure and function [22]. The mice initially underwent parasternal long and short-axis two-dimensional (2D) echocardiography at the level of the cardiac papillary muscles for the preliminary assessment of cardiac morphology. Then, a 2D guided M-mode trace was performed that crossed the left ventricle, and the morphological parameters were analyzed.

Invasive hemodynamic parameters were captured using a 1F microtip pressure-volume catheter (PVR 1045) (Millar Instruments, Houston, TX, USA) that linked to a PowerLab/4SP acquisition system (ADInstruments Inc., Sydney, Australia) [23]. The right carotid artery was surgically dissected, and then the cardiac catheter was inserted into the left ventricle through the isolated artery for the measurement of the left intraventricular pressure. Data were acquired by study investigators who were unaware of the assignment of the mouse groups.

#### Detection of biochemical markers of cardiac myocyte injury

Serum concentrations of cardiac troponin T (cTnT), creatine kinase myocardial band (CK-MB) isoenzyme and lactate dehydrogenase (LDH) were quantified using assay kits, as previously described [22]. The levels of malondialdehyde (MDA) and the antioxidant, glutathione (GSH), and the activity of superoxide dismutase (SOD) and NADPH oxidase (NOX) were assessed using the SpectraMax® 190 Microplate Reader (Molecular Devices, San Jose, CA, USA) [24]. The levels of 4-hydroxynonenal (4-HNE) protein adducts and 3-nitrotyrosine (3-NT) were measured according to the manufacturer's instructions.

#### TUNEL staining and detection of caspase-3 activity

Cell apoptosis was detected by the TUNEL assay, according to the manufacturer's instructions, and the fluorescence staining was imaged using an Olympus DX51 fluorescence microscope (Olympus, Tokyo, Japan) with the evaluation of more than five fields per heart (6 mouse hearts per group), as previously described [25]. The percentage of TUNEL-positive cells and the ratio of TUNEL-positive to 4,6-diamidino-2-phenylindole (DAPI)-positive cells were counted and calculated independently. Caspase-3 activity was measured using a commercial colorimetric assay kit (BF3100) (R&D Systems, Minneapolis, MN, USA), as previously reported [18]. Briefly, mouse hearts or cultured cells were harvested in the lysis buffer and centrifuged at 10,000g for 1 minute with the collection of the supernatant, and detection was performed at 405 nm by a SpectraMax 190 microplate reader (Molecular Devices, San Jose, CA, USA) [18].

#### Quantitative real-time polymerase chain reaction (qRT-PCR) and immunoblot analysis

Total RNA was extracted from the left ventricles of murine hearts or H9C2 cells using TRIzol reagent, and qRT-PCR was performed using PerfeCTa SYBR Green Supermix on an ABI 7500 Real-Time PCR Instrument (ThermoFisher Scientific, Waltham, MA, USA) [26]. Gene expression was adjusted against GAPDH or U6. The primer sequences are shown in Table 1.

Total proteins were extracted by the RIPA lysis, and the concentrations were calculated with a BCA protein assay kit. The proteins were transferred onto polyvinylidene difluoride (PVDF) membranes (ThermoFisher Scientific, Waltham, MA, USA) after electrophoresis at 70V for 30 minutes and 110V for 1.5 hours. After blocking with 5% dried skimmed milk powder for 2 hours at room temperature, the membranes were incubated with the primary antibodies overnight at 4°C, followed by incubation with the secondary antibody at room temperature for 1 hour, as previously described [27]. The membranes were scanned using the ChemiDoc™ Touch Imaging System (Bio-Rad, Hercules, CA, USA) and analyzed using Image Lab Software (Bio-Rad, Hercules, CA, USA).

### H9C2 cell culture and treatment

H9C2 rat cardiac myocytes were obtained from American Type Culture Collection (ATCC) (Manassas, VA, USA) and were cultured in Dulbecco's modified Eagle's medium (DMEM) containing 10% FBS [28,29]. After resynchronization in serum-free medium for 16 hours, cells were then transfected with the miR-143 antagomir (50 nM), the miR-143 agomir (50 nM), or their negative controls using Lipofectamine RNAiMAX (Invitrogen, Carlsbad, CA, USA) for 24 hours, after which, the cells were stimulated by doxorubicin (1 µM) for another 24 hours. The AKT inhibitor, MK2206 (1 µM) was added to the medium for 24 hours to inhibit AKT, and AKT overexpression was achieved by pre-infecting the cells with Ad-ca.Akt, according to the methods previously reported [30].

### DCFH-DA staining and the CCK-8 assay for cell viability

After removing the medium, H9C2 cells were incubated with serum-free medium containing DCFH-DA (10 µM) for additional 30 minutes, which were then observed using an Olympus fluorescence microscope (Olympus, Tokyo, Japan) [3]. The CCK-8 assay was performed to determine cell viability previously described [31]. The study investigators who analyzed the data were unaware of the assignment of the mouse groups.

### Statistical analysis

Data were expressed as the mean±standard deviation (SD) with 95% confidence intervals (CIs). Differences between two groups were compared using the two-tailed Student's t-test. One-way analysis of variance (ANOVA) was followed by the Student-Newman-Keuls (SNK) test for multiple comparison testing. Statistical analysis was performed using SPSS version 23.0 software (IBM, Chicago, IL, USA). A P-value <0.05 was considered to be statistically significant.

## Results

### Inhibition of microRNA-143 (miR-143) reduced doxorubicin-induced cardiac toxicity in the mouse model

As shown in Figure 1A, doxorubicin treatment significantly up-regulated miR-143 expression *in vivo* and *in vitro*, which was consistent with the findings from previous studies [14,17]. In this study, mice were treated with the miR-143 antagomir to inhibit endogenous miR-143 expression in mouse hearts, to determine the role of miR-143 in doxorubicin-induced cardiac toxicity (Figure 1B).

Doxorubicin treatment resulted in significant cardiac dysfunction, as determined by the impaired cardiac fractional shortening (FS) and stroke volume, which were improved by miR-143 inhibition (Figure 1C–1E). Doxorubicin treatment also caused whole-body cachexia, characterized by the loss of body-weight [3]. Also miR-143 inhibition preserved the body mass in the presence of doxorubicin toxicity, but it did not affect body-weight in normal untreated mice (Figure 1F). Heart weight was significantly reduced in the doxorubicin-treated mice, which significantly improved after miR-143 inhibition (Figure 1G). Also, the serum concentrations of cardiac troponin T (cTnT), lactate dehydrogenase (LDH), and creatine kinase myocardial band (CK-MB) isoenzyme, which are markers for myocardial injury, were significantly upregulated in mice with doxorubicin administration compared with that in the normal saline (NS) or control group, which were significantly reduced by the miR-143 antagomir (Figure 1H–1J). Also, miR-143 inhibition reduced doxorubicin-induced mortality in the mice (Figure 1K). These findings showed that miR-143 inhibition reduced doxorubicin-induced cardiac toxicity in the mouse model.

### MiR-143 overexpression increased cardiac injury in response to doxorubicin toxicity

To determine the role of miR-143, mice were treated with the miR-143 agomir to increase the miR-143 levels *in vivo* (Figure 2A). Functional parameters showed that miR-143 overexpression increased doxorubicin-induced cardiac dysfunction (Figure 2B). We also found that bodyweight and heart weight in miR-143 agomir-treated mice were further reduced in response to doxorubicin toxicity compared with that in mice treated with agomir control (Figure 2C, 2D). Also, serum concentrations of cTnT, LDH and CK-MB were further increased after treatment with the miR-143 agomir in the presence of doxorubicin treatment, indicating that miR-143 overexpression increased cardiac injury induced by doxorubicin (Figure 2E).

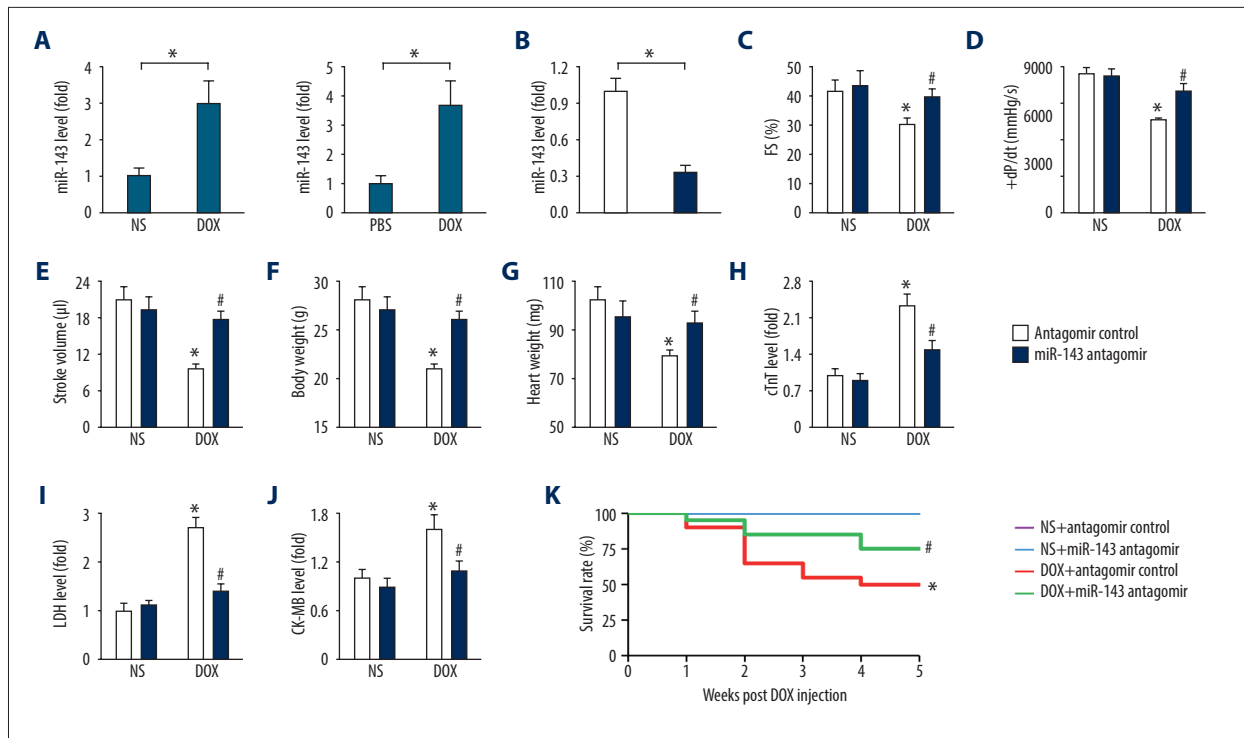


**Figure 1.** Inhibition of microRNA-143 (miR-143) reduced doxorubicin-induced cardiac toxicity in mice. (A) The expression of miR-143 in mouse hearts and H9C2 cells (n=6). (B) Statistical findings of the efficacy of the miR-143 antagomir (n=6). (C–E) Fractional shortening (FS), +dP/dt, and stroke volume in the mouse groups (n=8). (F, G) Bodyweight and heart weight in the mouse groups (n=6). (H–J) Serum concentrations of cardiac troponin T (cTnT), lactate dehydrogenase (LDH), and creatine kinase myocardial band (CK-MB) isoenzyme in the mouse groups with or without miR-143 antagomir treatment (n=20). Data are presented as the mean±standard deviation (SD) with the 95% confidence interval (CI). \* P<0.05 versus the normal saline (NS)+antagomir control group. # P<0.05 versus the doxorubicin+antagomir control group. In Figure A and B, \* P<0.05 versus the matched group.

### MiR-143 regulated doxorubicin-induced oxidative stress and myocardial apoptosis *in vivo*

Increased production of ROS is an important initiating mechanism in doxorubicin-induced cardiac toxicity, which results in myocardial cell loss [5]. As shown in Figure 3A, miR-143 inhibition significantly reduced lipid peroxidation and restored GSH levels in the myocardium (Figure 3A). 4-HNE is also regarded as a stable biomarker for lipid peroxidation, whereas 3-NT is a marker of protein oxidation produced upon the nitration of protein residues. The increased levels of 4-HNE, and 3-NT were observed in doxorubicin-treated mouse hearts and was reduced by miR-143 inhibition (Figure 3B). Also, doxorubicin-triggered down-regulation of SOD activity and upregulation of NOX activity were both attenuated in miR-143 antagomir-treated hearts (Figure 3C, 3D). Myocardial apoptosis is a key feature in doxorubicin-induced cardiac toxicity that contributes to the occurrence of cardiac impairment.

Quantitative real-time polymerase chain reaction (qRT-PCR) data showed that miR-143 antagomir administration significantly

increased BCL-2 gene expression while suppressed BAX level and the activity of caspase-3 was also reduced by miR-143 inhibition (Figure 3E, 3F). In line with the molecular alteration, TUNEL-positive cells were also reduced in mice with miR-143 antagomir treatment (Figure 3G, 3H), which were further confirmed by the expression of apoptosis-related proteins (Figure 3I). The use of the miR-143 agomir showed that miR-143 overexpression further reduced SOD activity and increased NOX activity in the presence of doxorubicin (Figure 3). The level of oxidative stress was assessed by the increased concentrations of MDA, 4-HNE, and 3-NT and was increased in mouse hearts when miR-143 was overexpressed (Figure 3K). Also, caspase-3 activity induced by doxorubicin treatment was significantly increased by the miR-143 agomir (Figure 3L). These data supported that miR-143 was involved in myocardial apoptosis and oxidative stress in the mouse model of doxorubicin-induced cardiac toxicity.

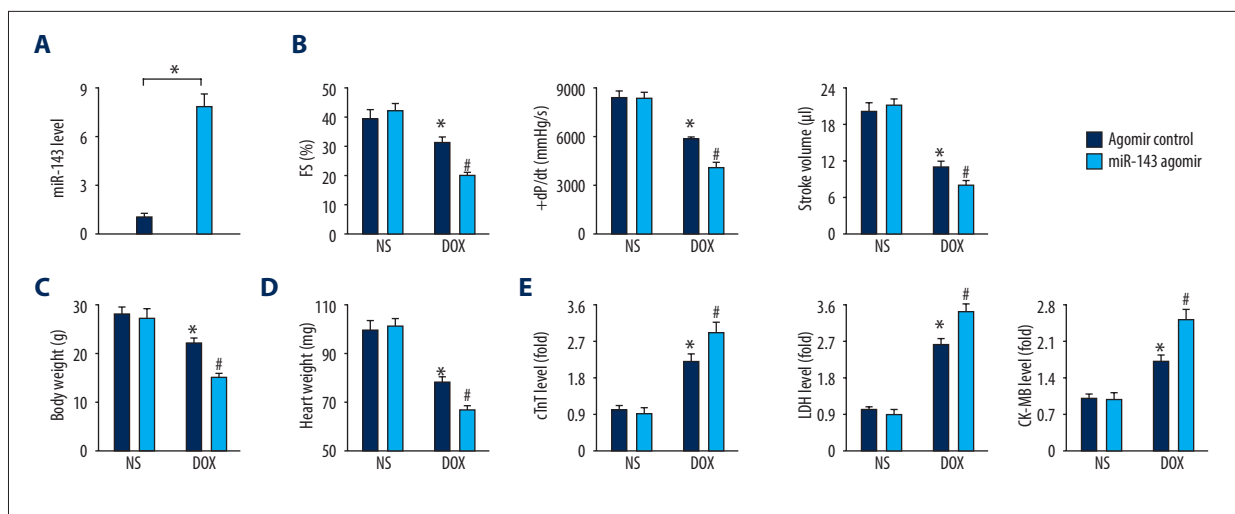


**Figure 2.** Upregulation of microRNA-143 (miR-143) increased cardiac injury in response to doxorubicin toxicity. **(A)** Statistical findings on the efficacy of the miR-143 agomir in the mouse groups (n=6). **(B)** Functional parameters of murine hearts in the mouse groups (n=6). **(C, D)** Bodyweight and heart weight detection in the mouse groups (n=8). **(E)** Serum concentrations of cardiac troponin T (cTnT), lactate dehydrogenase (LDH) and creatine kinase myocardial band (CK-MB) isoenzyme in the mouse groups (n=6). Data are presented as the mean±standard deviation (SD) with the 95% confidence interval (CI). \* P<0.05 versus the normal saline (NS)+antagomir control group. # P<0.05 versus the doxorubicin+antagomir control group. In Figure A, \* P<0.05 versus the matched group.

### miR-143 regulated oxidative stress and myocardial apoptosis in response to doxorubicin *in vitro*

To assess the role of miR-143 in doxorubicin-induced cardiac toxicity, miR-143 antagomir, agomir, or the negative controls were used *in vitro*. Dichloro-dihydro-fluorescein diacetate (DCFH-DA) staining indicated that miR-143 antagomir significantly reduced doxorubicin-induced ROS generation, which was further approved by reduced MDA production and increased GSH level (Figure 4A, 4B). Also, the study findings showed that miR-143 inhibition restored the abnormal SOD and NOX activities induced by doxorubicin treatment (Figure 4C, 4D). Data from qRT-PCR and immunoblot analysis of BCL-2, BAX, and caspase-3 detection both implied that miR-143 antagomir treatment significantly inhibited doxorubicin-induced myocardial apoptosis (Figure 4E, 4F). The detection of caspase-3 activity and cell viability further corroborated that miR-143 inhibition could prevent doxorubicin-induced cell loss (Figure 4G, 4H). The *in vivo* data were supported by the finding that the use of the miR-143 agomir increased doxorubicin-induced oxidative stress, as evidenced by the DCFH-DA staining, increased MDA content, NOX activity and reduced SOD activity (Figure 4I–4K). Doxorubicin-induced myocardial apoptosis was also enhanced by miR-143 agomir, characterized by the increased caspase-3 activity and reduced cell viability (Figure 4L, 4M).

### miR-143 increased the AKT signaling pathway *in vitro*

The underlying mechanism that were responsible for the effects of miR-143 were investigated in doxorubicin-induced cardiac toxicity *in vitro*. Previous studies showed that miR-143 could target sprouty3 and caused its degradation, and thereby activating its downstream P38, ERK pathways [32]. Also, a previous study has shown that upregulation of miR-143 also inhibited PKC $\epsilon$  expression and reduced the cardioprotective effects on myocardial infarction [18]. However, in the present study, the use of the miR-143 antagomir did not affect the protein levels of P38, ERK and PKC $\epsilon$  in the presence of doxorubicin (Figure 5A, 5B).

Jordan et al. found that miR-143 overexpression resulted in the down-regulation of oxysterol-binding-protein-related protein 8 (ORP8) and impaired AKT phosphorylation and that miR-143 down-regulation promoted AKT activation [33]. The findings from the present study supported these previous findings, as the miR-143 antagomir reduced doxorubicin-induced inactivation of AKT, whereas miR-143 overexpression further reduced AKT phosphorylation in the presence of doxorubicin (Figure 5A–5C). To determine the protective role of miR-143 antagomir was mediated by AKT activation, cells were pretreated with the AKT inhibitor, MK2206. As shown in Figure 5D, 5E, miR-143 inhibition-mediated down-regulation of MDA and upregulation of GSH were abolished by AKT inhibition. Also, the inhibitory effects on caspase-3 activity and cell death were also retarded in the presence of MK2206 (Figure 5F, 5G).

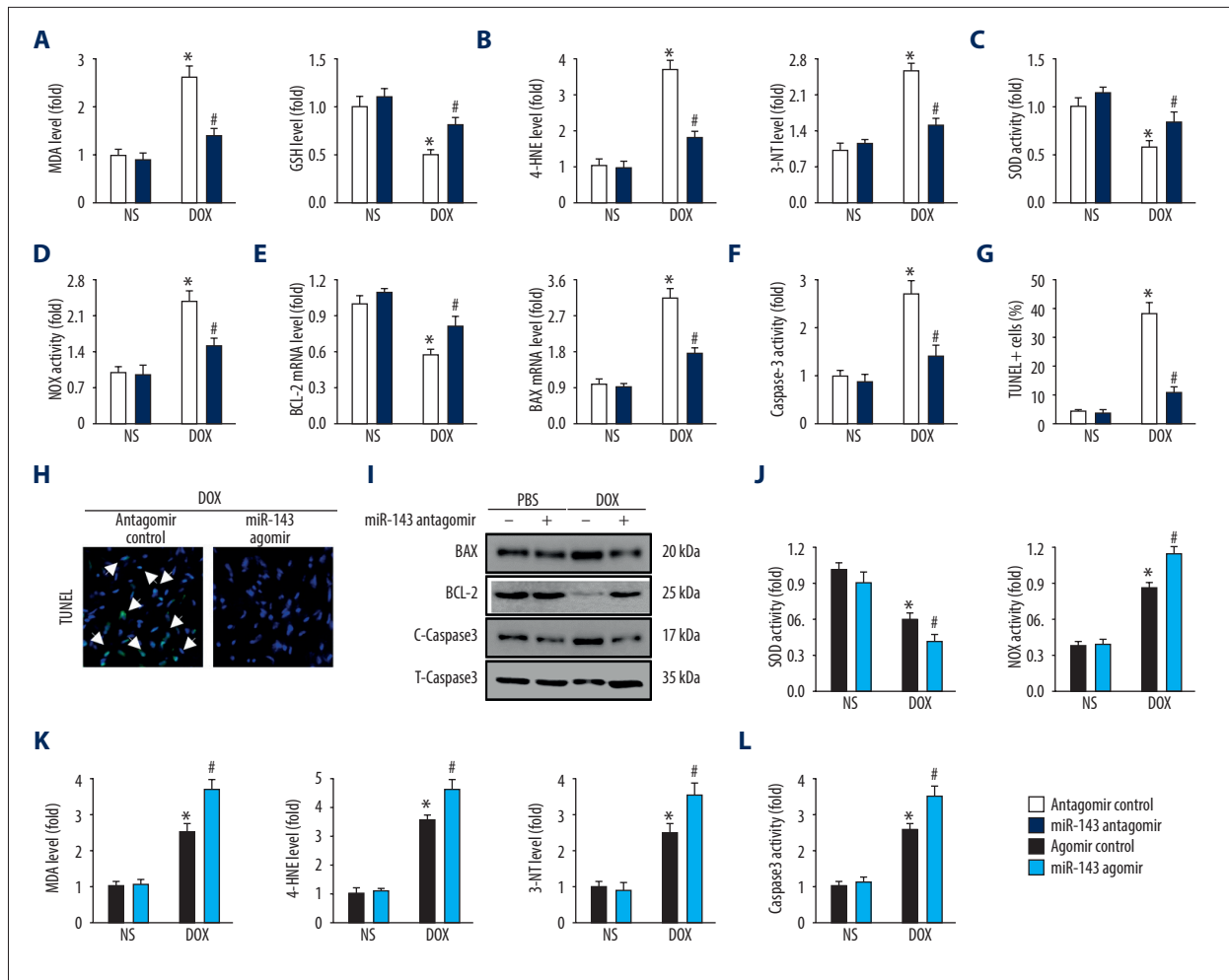


**Figure 3.** MicroRNA-143 (miR-143) regulated doxorubicin-induced oxidative stress and myocardial apoptosis *in vivo*. (A) Malondialdehyde (MDA) and glutathione (GSH) levels in the hearts in the mouse groups (n=6). (B) 4-hydroxynonenal (4-HNE) and 3-nitrotyrosine (3-NT) levels in the hearts in the mouse groups (n=6). (C, D) Superoxide dismutase (SOD) and NADPH oxidase (NOX) activities in the hearts in the mouse groups (n=6). (E) The relative mRNA levels of BCL-2 and BAX in the hearts in the mouse groups (n=8). (F) Caspase-3 activity in the hearts in the mouse groups (n=6). (G, H) Representative TUNEL images and the statistical analysis of TUNEL-positive cells in the mouse groups (n=6). (I) Representative immunoblot images in the mouse groups (n=6). (J) SOD and NOX activities in the hearts in the mouse groups (n=6). (K) MDA, 4-HNE, and 3-NT production in the hearts in the mouse groups (n=6). (L) The findings of caspase-3 activity in the mouse groups (n=6). Data are presented as the mean±standard deviation (SD) with the 95% confidence interval (CI). \* P<0.05 versus the normal saline (NS)+antagomir control group. # P<0.05 versus the doxorubicin+antagomir control group.

However, AKT activation significantly reduced the effects of the miR-143 agomir, which increased oxidative stress and myocardial apoptosis. These effects were shown by reduced MDA production, reduced caspase-3 activity, and increased cell viability (Figure 5H–5J). The efficacy of Ad-ca. Akt was shown by the immunoblot, indicating an increase of AKT phosphorylation (Figure 5K). These results showed that miR-143 was essential for doxorubicin-induced oxidative stress and myocardial apoptosis by regulating the AKT pathway *in vitro*.

#### AKT modulation reversed the effect of miR-143 on doxorubicin-induced cardiac toxicity *in vivo*

Consistent with the *in vitro* data, MK2206 treatment significantly reduced miR-143 inhibition-mediated protective effect in doxorubicin-treated mice, as reflected by the increased levels of caspase-3 activity, MDA, and 4-HNE content (Figure 6A, 6B). Functional parameters showed that the improved FS and stroke volume in mice assigned to the doxorubicin and miR-143 antagomir group were significantly reduced by AKT inhibition (Figure 6C). Further detection of cTnT and LDH showed that the use of the miR-143 antagomir resulted in the loss of the

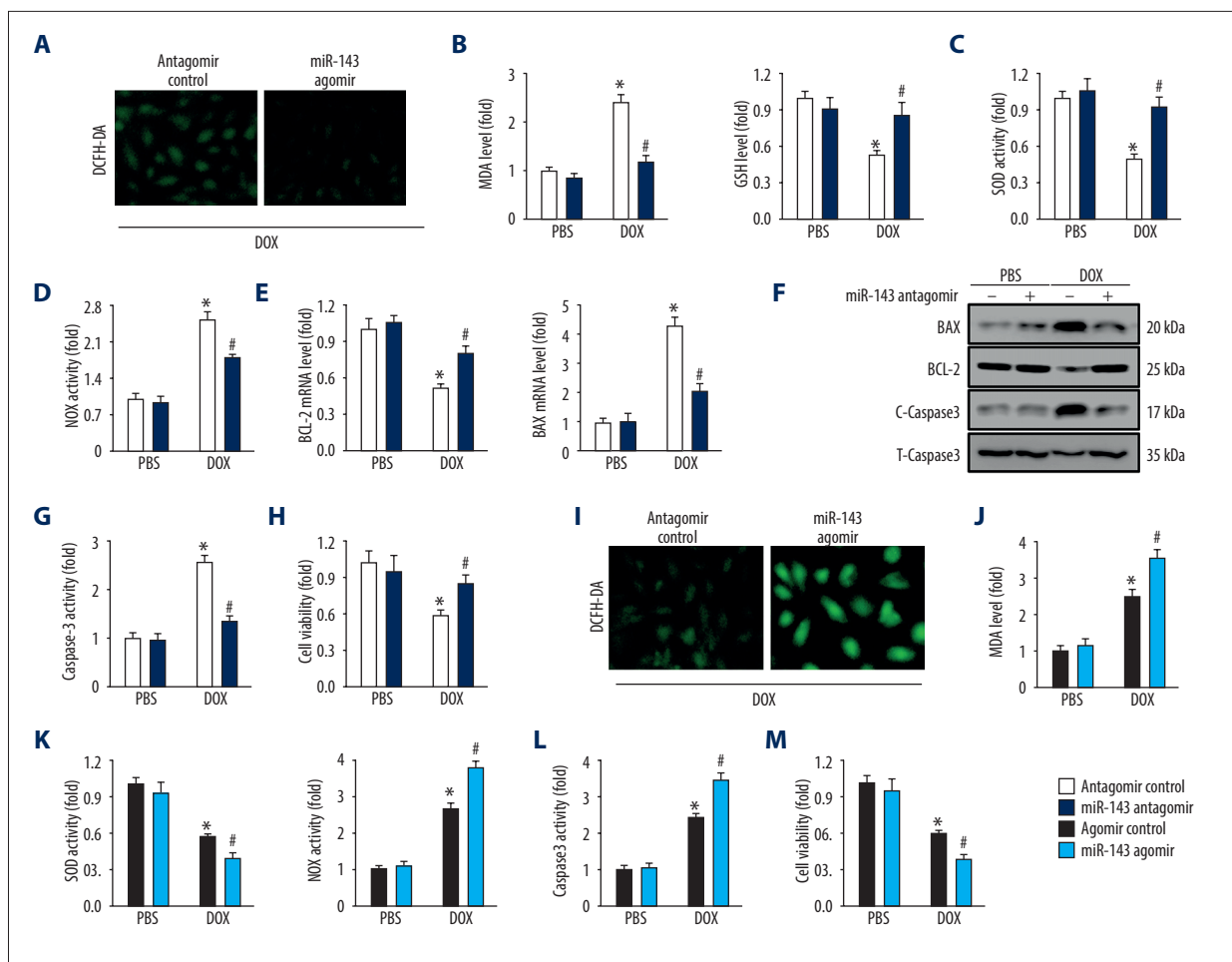


**Figure 4.** MicroRNA-143 (miR-143) regulated oxidative stress and myocardial apoptosis in response to doxorubicin *in vitro*. (A) Representative images of dichloro-dihydro-fluorescein diacetate (DCFH-DA) staining of H9C2 cells (n=6). (B) Malondialdehyde (MDA) and glutathione (GSH) levels in cultured H9C2 cells (n=6). (C, D) Superoxide dismutase (SOD) and NADPH oxidase (NOX) activities in cultured H9C2 cells (n=6). (E) The relative mRNA levels about BCL-2 and BAX in cells (n=8). (F) Representative images of immunoblots (n=6). (G) Data on caspase-3 activity in cells (n=6). (H) Cell viability detected using the cell counting kit-8 (CCK-8) assay (n=6). (I) Representative images of DCFH-DA staining (n=6). (J) MDA production in cultured H9C2 cells (n=6). (K) SOD and NOX activities in H9C2 cells (n=6). (L) Quantitative data on caspase-3 activity in H9C2 cells (n=6). (M) Statistical analysis of cell viability *in vitro* (n=6). Data are presented as the mean±standard deviation (SD) with the 95% confidence interval (CI). \* P<0.05 versus the normal saline (NS)+antagomir control group. # P<0.05 versus the doxorubicin+antagomir control group.

inhibitory effect on doxorubicin-induced myocardial injury after AKT inhibition (Figure 6D). The effects of the miR-143 agonist on myocardial apoptosis and oxidative stress were also prevented in mice with AKT activation, as confirmed by the reduced levels of MDA and 4-HNE, and reduced the activity of caspase-3 (Figure 6E, 6F). The increased cardiac dysfunction associated with the miR-143 agomir was abolished after Ad-ca.Akt injection (Figure 6G). The detection of serum levels of cTnT further showed that AKT activation reversed the toxic effects of the miR-143 agomir on doxorubicin-induced myocardial injury in the mouse model (Figure 6H).

## Discussion

Doxorubicin is a broad-spectrum chemotherapeutic agent that is commonly used for the treatment of advanced-stage human cancers, but cardiac toxicity is associated with its use [2]. Although efforts have been made to reduce doxorubicin-induced cardiac toxicity, progress has been limited by the lack of understanding of the complex pathogenesis of these effects. The findings from the present study showed that microRNA-143 (miR-143) was involved in the progression of doxorubicin-induced cardiac toxicity in the mouse model. In this study, miR-143 inhibition reduced doxorubicin-induced cardiac toxicity in the mouse model, whereas miR-143 overexpression



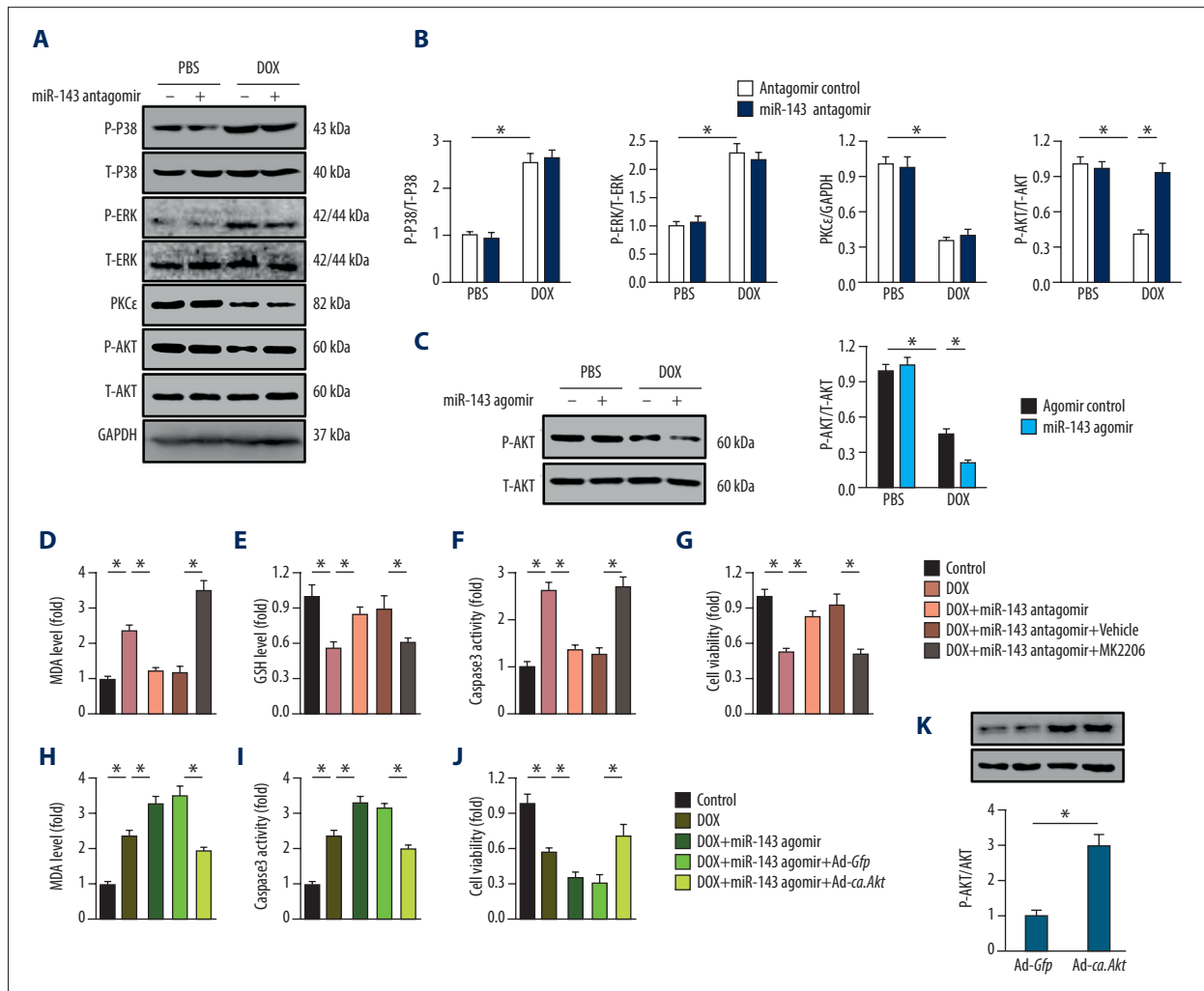


**Figure 5.** MicroRNA-143 (miR-143) and the AKT signaling pathway *in vitro*. **(A, B)** Protein expression and the statistical analysis in H9C2 cells (n=6). **(C)** Representative images of immunoblots and quantitative data (n=6). **(D, E)** Malondialdehyde (MDA) and glutathione (GSH) levels in H9C2 cells (n=6). **(F, G)** Quantitative data on caspase-3 activity and cell viability in H9C2 cells (n=6). **(H)** MDA production (n=6). **(I, J)** Caspase-3 activity and cell viability detection in H9C2 cells (n=6). **(K)** The efficacy of the Ad-ca.Akt confirmed by immunoblot (n=6). Data are presented as the mean±standard deviation (SD) with the 95% confidence interval (CI). \* P<0.05 versus the matched group.

increased doxorubicin-induced myocardial apoptosis and oxidative stress. Also, the findings from this study showed that miR-143 acted through the AKT signaling pathway, and AKT modulation reversed the effect of miR-143 on doxorubicin-induced cardiac toxicity *in vivo* and *in vitro*. These findings provided a novel insight into the pathogenesis of doxorubicin-induced cardiac toxicity and the involvement of miR-143 in the mouse model of doxorubicin-induced cardiac toxicity.

Several cellular mechanisms have been proposed to be involved in the progression of doxorubicin-induced myocardial injury. Oxidative stress due to increased generation of reactive oxygen species (ROS) has been identified as the primary factor associated with the progression of doxorubicin-induced

cardiac dysfunction [3,10]. Previous studies showed that indicators of oxidative stress could be detected within three hours in doxorubicin-treated heart tissue samples [34]. Mitochondria are the main source of intracellular ROS and are also the most extensively injured subcellular organelles in doxorubicin-induced cardiac toxicity [35,36]. Doxorubicin can be enriched in the inner membrane of mitochondria, where they bind to cardiolipin to disrupt normal mitochondrial metabolism and ATP synthesis [6].

In response to oxidative stress, cells have evolved to develop a unique antioxidant mechanism to reduce ROS levels and improve cell survival. Among these mechanisms, superoxide dismutase (SOD) can catalytically reduce  $O_2^-$  to hydrogen peroxide,

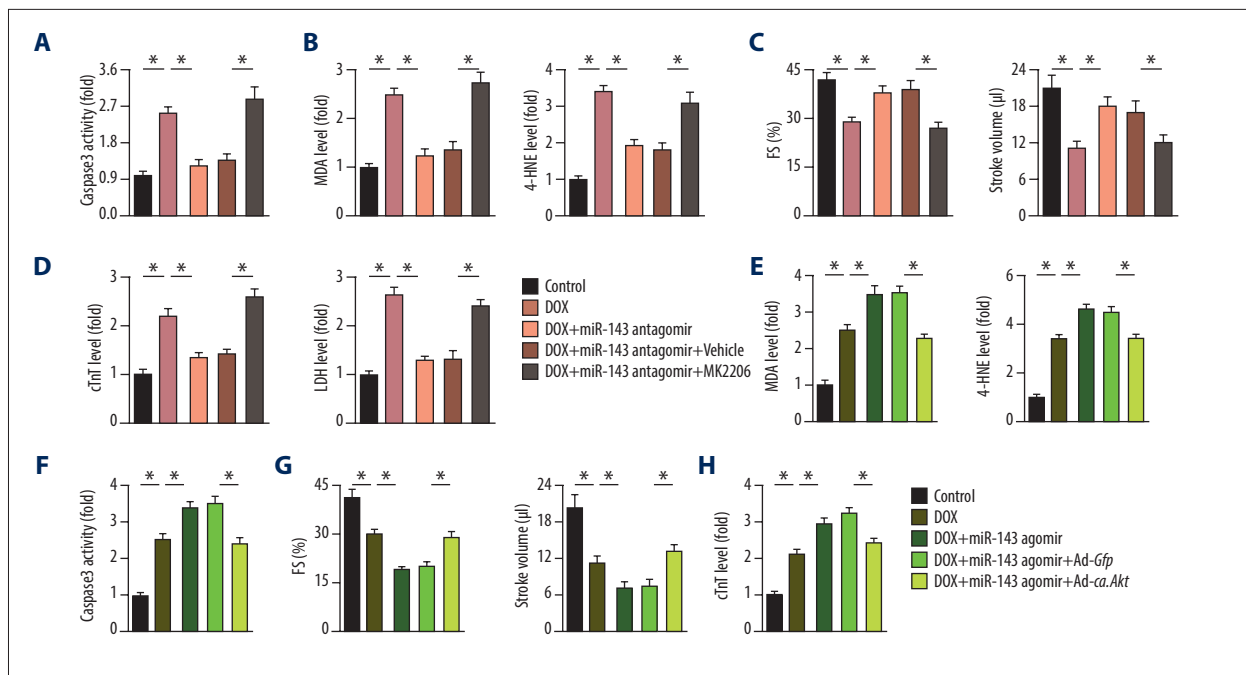


**Figure 6.** AKT inhibition reversed the effect of microRNA-143 (miR-143) on doxorubicin-induced cardiac toxicity *in vivo*. (A) Quantitative result of caspase-3 activity in murine hearts (n=6). (B) Malondialdehyde (MDA) and 4-hydroxynonenal (4-HNE) production in the myocardium (n=6). (C) Cardiac fractional shortening (FS) and stroke volume in murine hearts (n=8). (D) Serum cardiac troponin T (cTnT) and lactate dehydrogenase (LDH) levels in mice in the study groups (n=6). (E) MDA and 4-HNE levels in murine hearts (n=6). (F) Data on caspase-3 activity in the myocardium (n=6). (G) FS and stroke volume in mice among groups (n=8). (H) Serum level of cTnT in mice (n=6). Data are presented as the mean±standard deviation (SD) with the 95% confidence interval (CI). \* P<0.05 versus the matched group.

and glutathione (GSH) catalyzes the degradation of hydrogen peroxide and other peroxides, thereby ensuring the redox homeostasis for normal cell physiology [10]. Unrestrained ROS generation may cause lipid and protein peroxidation and disrupt cell membrane structural integrity, leading to the activation of apoptotic cascades and ultimately causing doxorubicin-induced cardiac impairment [37]. The findings from the present study showed that miR-143 inhibition protected the cardiac myocyte, whereas miR-143 overexpression increased oxidative stress and myocardial apoptosis in the mouse model of doxorubicin-induced cardiac toxicity.

AKT is a serine/threonine protein kinase that has a critical node in regulating the cell cycle, and in cell survival and proliferation [30,38]. Previous studies showed that AKT was inactivated by doxorubicin administration in heart samples, and AKT activation could promote cardiomyocyte survival and reduce doxorubicin-induced cardiac impairment [39]. In addition to the role in regulating cell survival, AKT also plays critical roles in reducing oxidative stress [40]. Dai and colleagues showed that AKT activation could inhibit glycogen synthase kinase 3β (GSK3β) activation, which subsequently promoted Nrf2 nuclear retention by increasing Fyn nuclear export [41]. Zhang et al. previously showed that the activation of AKT could reduce

doxorubicin-induced oxidative damage by reducing GSK3β/FYN-mediated Nrf2 nuclear export and degradation [3]. Lien et al. showed that AKT activation stimulated GSH biosynthesis and enhanced the total antioxidant capacity [42]. The findings from the present study showed that the effects of doxorubicin-induced oxidative damage due to miR-143 inhibition were significantly reduced with AKT inhibition and that AKT activation prevented miR-143 agomir-mediated increase in doxorubicin-induced oxidative damage.

However, the detailed molecular mechanisms involved in the interaction between miR-143 and AKT phosphorylation were not identified in the present study. Previous studies showed that microRNAs could bind to the 3'-untranslated regions (UTR) of mRNAs and inhibit gene expression at the post-transcriptional level. Therefore, the effect of miR-143 on AKT phosphorylation might involve the upstream molecular AKT pathway. In addition to acute cardiac toxicity, doxorubicin treatment is associated with chronic cardiac toxicity in approximately 1.7% of patients [43]. Therefore, further studies are required, including future clinical studies, to determine the role of miR-143 on doxorubicin-induced chronic cardiac toxicity.

## Conclusions

This study aimed to investigate the effects and possible molecular mechanisms of miR-143 on oxidative stress and myocardial cell apoptosis in a mouse model of doxorubicin-induced cardiac toxicity. In a mouse model of doxorubicin-induced cardiac toxicity, miR-143 increased oxidative stress and myocardial cell apoptosis following doxorubicin treatment by inhibiting AKT.

## References:

1. Silber JH, Barber G: Doxorubicin-induced cardiotoxicity. *N Engl J Med*, 1995; 333: 1359–60
2. Zhang S, Liu X, Bawa-Khalfe T et al: Identification of the molecular basis of doxorubicin-induced cardiotoxicity. *Nat Med*, 2012; 18: 1639–42
3. Zhang X, Hu C, Kong CY et al: FNDC5 alleviates oxidative stress and cardiomyocyte apoptosis in doxorubicin-induced cardiotoxicity via activating AKT. *Cell Death Differ*, 2019 [Epub ahead of print]
4. Zhu SG, Kukreja RC, Das A et al: Dietary nitrate supplementation protects against Doxorubicin-induced cardiomyopathy by improving mitochondrial function. *J Am Coll Cardiol*, 2011; 57: 2181–89
5. Octavia Y, Tocchetti CG, Gabrielson KL et al: Doxorubicin-induced cardiomyopathy: From molecular mechanisms to therapeutic strategies. *J Mol Cell Cardiol*, 2012; 52: 1213–25
6. Goormaghtigh E, Chatelain P, Caspers J, Ruyschaert JM: Evidence of a complex between adriamycin derivatives and cardiolipin: possible role in cardiotoxicity. *Biochem Pharmacol*, 1980; 29: 3003–10
7. Gabisonia K, Prosdocimo G, Aquaro GD et al: MicroRNA therapy stimulates uncontrolled cardiac repair after myocardial infarction in pigs. *Nature*, 2019; 569: 418–22
8. Chaudhari U, Nemade H, Gaspar JA et al: MicroRNAs as early toxicity signatures of doxorubicin in human-induced pluripotent stem cell-derived cardiomyocytes. *Arch Toxicol*, 2016; 90: 3087–98
9. Horie T, Ono K, Nishi H et al: Acute doxorubicin cardiotoxicity is associated with miR-146a-induced inhibition of the neuregulin-ErbB pathway. *Cardiovasc Res*, 2010; 87: 656–64
10. Zhao L, Qi Y, Xu L et al: MicroRNA-140-5p aggravates doxorubicin-induced cardiotoxicity by promoting myocardial oxidative stress via targeting Nrf2 and Sirt2. *Redox Biol*, 2018; 15: 284–96
11. Deng L, Blanco FJ, Stevens H et al: MicroRNA-143 activation regulates smooth muscle and endothelial cell crosstalk in pulmonary arterial hypertension. *Circ Res*, 2015; 117: 870–83
12. Avalle L, Incarnato D, Savino A et al: MicroRNAs-143 and -145 induce epithelial to mesenchymal transition and modulate the expression of junction proteins. *Cell Death Differ*, 2017; 24: 1750–60
13. Fernandes T, Hashimoto NY, Magalhaes FC et al: Aerobic exercise training-induced left ventricular hypertrophy involves regulatory MicroRNAs, decreased angiotensin-converting enzyme-angiotensin ii, and synergistic regulation of angiotensin-converting enzyme 2-angiotensin (1–7). *Hypertension*, 2011; 58: 182–89
14. Zhang J, Sun Q, Zhang Z et al: Loss of microRNA-143/145 disturbs cellular growth and apoptosis of human epithelial cancers by impairing the MDM2-p53 feedback loop. *Oncogene*, 2013; 32: 61–69
15. Dou L, Zheng D, Li J et al: Methylation-mediated repression of microRNA-143 enhances MLL-AF4 oncogene expression. *Oncogene*, 2012; 31: 507–17
16. Kohlstedt K, Trouvain C, Boettger T et al: AMP-activated protein kinase regulates endothelial cell angiotensin-converting enzyme expression via p53 and the post-transcriptional regulation of microRNA-143/145. *Circ Res*, 2013; 112: 1150–58
17. Deacon DC, Nevis KR, Cashman TJ et al: The miR-143-adducin3 pathway is essential for cardiac chamber morphogenesis. *Development*, 2010; 137: 1887–96
18. Hong H, Tao T, Chen S et al: MicroRNA-143 promotes cardiac ischemia-mediated mitochondrial impairment by the inhibition of protein kinase Cepsilon. *Basic Res Cardiol*, 2017; 112: 60
19. Ma W, Ding F, Wang X et al: By targeting Atg7 microRNA-143 mediates oxidative stress-induced autophagy of c-Kit(+) mouse cardiac progenitor cells. *EBioMedicine*, 2018; 32: 182–91
20. Jeong SH, Kim HB, Kim MC et al: Hippo-mediated suppression of IRS2/AKT signaling prevents hepatic steatosis and liver cancer. *J Clin Invest*, 2018; 128: 1010–25
21. Ma ZG, Yuan YP, Zhang X et al: Piperine attenuates pathological cardiac fibrosis via PPAR-gamma/AKT pathways. *EBioMedicine*, 2017; 18: 179–87
22. Hu C, Zhang X, Wei W et al: Matrine attenuates oxidative stress and cardiomyocyte apoptosis in doxorubicin-induced cardiotoxicity via maintaining AMPKalpha/UCP2 pathway. *Acta Pharm Sin B*, 2019; 9: 690–701
23. Deshwal S, Forkink M, Hu CH et al: Monoamine oxidase-dependent endoplasmic reticulum-mitochondria dysfunction and mast cell degranulation lead to adverse cardiac remodeling in diabetes. *Cell Death Differ*, 2018; 25: 1671–85
24. Ma ZG, Yuan YP, Xu SC et al: CTRP3 attenuates cardiac dysfunction, inflammation, oxidative stress and cell death in diabetic cardiomyopathy in rats. *Diabetologia*, 2017; 60: 1126–37
25. Zhang X, Zhu JX, Ma ZG et al: Rosmarinic acid alleviates cardiomyocyte apoptosis via cardiac fibroblast in doxorubicin-induced cardiotoxicity. *Int J Biol Sci*, 2019; 15: 556–67
26. Mughal W, Martens M, Field J et al: Myocardin regulates mitochondrial calcium homeostasis and prevents permeability transition. *Cell Death Differ*, 2018; 25: 1732–48
27. Wang K, Ding R, Ha Y et al: Hypoxia-stressed cardiomyocytes promote early cardiac differentiation of cardiac stem cells through HIF-1alpha/Jagged1/Notch1 signaling. *Acta Pharm Sin B*, 2018; 8: 795–804
28. Prola A, Pires DSJ, Guilbert A et al: SIRT1 protects the heart from ER stress-induced cell death through eIF2alpha deacetylation. *Cell Death Differ*, 2017; 24: 343–56
29. Li Z, Song Y, Liu L et al: miR-199a impairs autophagy and induces cardiac hypertrophy through mTOR activation. *Cell Death Differ*, 2017; 24: 1205–13
30. Ma ZG, Zhang X, Yuan YP et al: A77 1726 (leflunomide) blocks and reverses cardiac hypertrophy and fibrosis in mice. *Clin Sci (Lond)*, 2018; 132: 685–99
31. Zhang X, Ma ZG, Yuan YP et al: Rosmarinic acid attenuates cardiac fibrosis following long-term pressure overload via AMPKalpha/Smad3 signaling. *Cell Death Dis*, 2018; 9: 102
32. Li C, Li J, Xue K et al: MicroRNA-143-3p promotes human cardiac fibrosis via targeting sprout3 after myocardial infarction. *J Mol Cell Cardiol*, 2019; 129: 281–92
33. Jordan SD, Kruger M, Willmes DM et al: Obesity-induced overexpression of miRNA-143 inhibits insulin-stimulated AKT activation and impairs glucose metabolism. *Nat Cell Biol*, 2011; 13: 434–46
34. Chaiswing L, Cole MP, St Clair DK et al: Oxidative damage precedes nitrate damage in adriamycin-induced cardiac mitochondrial injury. *Toxicol Pathol*, 2004; 32: 536–47
35. Zhang X, Zhang X, Zhang Y et al: Mitochondrial uncoupler triclosan induces vasorelaxation of rat arteries. *Acta Pharm Sin B*, 2017; 7: 623–29
36. Li J, Wang PY, Long NA et al: p53 prevents doxorubicin cardiotoxicity independently of its prototypical tumor suppressor activities. *Proc Natl Acad Sci USA*, 2019; 116(39): 19626–34
37. Battogtokh G, Choi YS, Kang DS et al: Mitochondria-targeting drug conjugates for cytotoxic, anti-oxidizing and sensing purposes: Current strategies and future perspectives. *Acta Pharm Sin B*, 2018; 8: 862–80
38. Zhao W, Qiu Y, Kong D: Class I phosphatidylinositol 3-kinase inhibitors for cancer therapy. *Acta Pharm Sin B*, 2017; 7: 27–37

## Conflict of interest

None.

39. Fan GC, Zhou X, Wang X et al: Heat shock protein 20 interacting with phosphorylated Akt reduces doxorubicin-triggered oxidative stress and cardiotoxicity. *Circ Res*, 2008; 103: 1270–79
40. Port J, Muthalagu N, Raja M et al: Colorectal tumors require NUA1 for protection from oxidative stress. *Cancer Discov*, 2018; 8: 632–47
41. Dai X, Yan X, Zeng J et al: Elevating CXCR7 improves angiogenic function of EPCs via Akt/GSK-3beta/Fyn-mediated Nrf2 activation in diabetic limb ischemia. *Circ Res*, 2017; 120: e7–23
42. Lien EC, Lyssiotis CA, Juvekar A et al: Glutathione biosynthesis is a metabolic vulnerability in PI(3)K/Akt-driven breast cancer. *Nat Cell Biol*, 2016; 18: 572–78
43. Von Hoff DD, Layard MW, Basa P et al: Risk factors for doxorubicin-induced congestive heart failure. *Ann Intern Med*, 1979; 91: 710–17